1394 *J. Chem. Eng. Data* **2007,** *52,* 1394−1400

Thermodynamics of Bismuth in the Molten Ag−Bi−Sn System

B. Brunetti,[†] D. Gozzi,* M. Iervolino, A. Latini, and V. Piacente

Dipartimento di Chimica, Università di Roma La Sapienza, Piazzale Aldo Moro, 5 - 00185 Roma, Italy

An experimental thermodynamic study has been performed on some liquid alloys of the ternary system Ag−Bi−Sn by making use of the torsion−effusion method. Through the measurement of the vapor pressure of Bi in thermodynamic equilibrium with the liquid phase, the Bi activity as a function of Bi atomic fraction, X_{Bi}, was obtained. Three ternary alloys having a fixed ratio $\rho = X_{Sn}/X_{Ag}$ (ρ: 0.095; 0.200; 0.333) were examined starting from the original alloy composition and changing X_{Bi} by selected short isothermal vaporizations of Bi. In this way, it was found that all the alloy tested had positive deviations from ideality. Some thermodynamic quantities were evaluated at $T = 1000$ K. They are Bi mixing partial molar quantities such as $\overline{\Delta_{mix}G_T}$(Bi), $\overline{\Delta_{mix}H_T}$(Bi), and $\overline{\Delta_{mix}S_T}$(Bi) and mixing integral molar quantities, i.e., $\Delta_{mix}G_T$(xs) and $\Delta_{mix}G_T$(re), which are excess and real, respectively.

1. Introduction

There is increasing technological interest for low melting point alloys suitable for use in soldering with lead-free materials. Worldwide, the presence of lead in the actual solders is considered very dangerous for the environment due to the huge amount of printed circuits and electronic devices to be recycled from municipal waste dumps. The European Community, the U.S. and Japan, as well as electronic industries launched initiatives to look for lead-free solders having physical, chemical, and technological properties comparable to or better than the Sn−Pb alloys in use. The COST Action 531,[1] started in March 2002 and to be finished in March 2007, has the main objective to increase the basic knowledge on possible alloy systems that can be used as lead-free solder materials. Furthermore, it should provide a scientific basis for a decision on which of these materials to use for different soldering purposes to replace the currently used lead-containing solders in the future. The whole COST 531 Action is now divided in four working groups, and at least one of them is mainly involved in the experimental thermodynamics of the selected alloys.

Among some binary alloys and several ternary alloys such as Ag−Bi−Sn, Ag−Cu−In, Ag−Cu−Sn, Ag−Sn+(Cu, Ni, Au, Pd), In−Sn−X, Ag−In−Sn+(Ni, Pd), Bi−Sn−X, and Sn−Zn−X (where X is other metals such as Ag, Au, Cu, Ni, Pd, and Sb) that have been proposed, Bi−In−Sn[2] was recently studied by our group, and a Ag−Bi−Sn alloy is considered in the present work. A few experimental constitutional[3] and thermodynamic[4−8] data on this system can be found in the literature along with some modeling[9] and assessment.[10] Therefore, the scope of the present work is to explore the thermodynamic behavior of the above liquid alloy at different compositions by determining the Bi activity. This was done by making use of the torsion−effusion (T−E) technique,[2,11] which has been practiced extensively in our laboratory.

2. Experimental

2.1. Alloy Preparation and Characterization. The metals used were bismuth, silver (both 99.999 mass % purity, MaTeck GmbH, Julich, Germany), and tin (99.999 mass % purity, Newmet Kock, Waltham Abbey, U.K.).

The alloys, each with a total weight of ≈ 5 g, were prepared by induction melting in alumina crucibles under argon flux. All the samples, enclosed under a vacuum in flame-sealed Pyrex ampoules, were annealed for one week at 200 °C in a resistance furnace and then air-cooled.

Optical and electronic metallographic examination was carried out on all samples. Light optical microscopy, scanning electron microscopy (SEM), and electron probe microanalysis (EPMA) based on energy dispersive X-ray spectroscopy were used to check the overall composition of the samples and to analyze the coexisting phases.

The microstructure of the alloys was investigated after preparing smooth surfaces of the specimen; the compositional contrast between the various phases has been observed by means of a back-scattered electron detector (BSE). For quantitative EPMA, the samples were analyzed at 20 kV acceleration voltage using cobalt as the standard for calibration of the beam current, gain, and resolution of the spectrometer. Finally, the X-ray intensities were corrected for ZAF (Z absorption fluorescence) effects using pure elements as standards.

2.2. Torsion−Effusion Method. The total vapor pressures above the liquid alloys were measured by the torsion−effusion method. These pressures inside the effusion cell are practically equal to the bismuth partial pressure, p_{Bi}, because this element is decidedly the most volatile species in the alloy. For example, the vapor pressure ratios[12] of p_{Bi}/p_{Ag} and p_{Bi}/p_{Sn} at 1000 K are about $3 \cdot 10^3$ and $2 \cdot 10^5$, respectively. The assembly used was substantially the same as that described in detail elsewhere.[11,13] The torsion apparatus is appropriately suspended from a Cahn 1000 vacuum electrobalance so that, during the vaporization of a sample, its weight loss was measured simultaneously. In this study, a conventional torsion pyrophyllite cell with 1.0 mm nominal diameter of both effusion holes was used. As usual, the cell constant value, K_α, necessary to convert the measured torsion angles of the assembly, α, to pressure data, was

---

* Corresponding author. E-mail: daniele.gozzi@uniroma1.it. COST 531, Lead-free Solder Materials, Management Committee Member.

[†] CNR-ISMN-sez.Roma1, Dipartimento di Chimica, Università di Roma La Sapienza.

10.1021/je7000914 CCC: $37.00

Table 1. Experimental Total Vapor Pressure, p_{tot}, above Binary Alloy $Ag_{10}Bi_{90}$

run #1		run #2		run #3		run #4		run #5		run #6		run #7		run #8		run #9	
T/K	$\log(p_{tot}/Pa)$	T/K	$\log(p_{tot}/Pa)$	T/K	$\log(p_{tot}/Pa)$	T/K	$\log(p_{tot}/Pa)$	T/K	$\log(p_{tot}/Pa)$	T/K	$\log(p_{tot}/Pa)$	T/K	$\log(p_{tot}/Pa)$	T/K	$\log(p_{tot}/Pa)$	T/K	$\log(p_{tot}/Pa)$
876	−0.77	909	−0.47	905	−0.42	895	−0.63	907	−0.53	880	−0.90	907	−0.67	895	−0.90	922	−0.63
892	−0.59	919	−0.29	915	−0.33	910	−0.47	917	−0.42	890	−0.77	910	−0.59	905	−0.77	928	−0.56
915	−0.29	929	−0.20	925	−0.20	917	−0.37	927	−0.26	900	−0.59	913	−0.53	915	−0.59	932	−0.53
925	−0.17	943	0.03	935	−0.05	927	−0.23	940	−0.09	908	−0.53	915	−0.53	921	−0.53	939	−0.42
934	−0.07	954	0.13	945	0.03	937	−0.14	950	−0.01	917	−0.47	920	−0.47	925	−0.47	943	−0.37
945	0.04	963	0.26	957	0.17	950	0.03	960	0.10	926	−0.33	926	−0.42	931	−0.42	949	−0.31
953	0.13	973	0.34	965	0.26	956	0.12	970	0.23	936	−0.20	929	−0.37	935	−0.37	954	−0.28
963	0.22	981	0.45	977	0.34	967	0.20	980	0.31	946	−0.12	934	−0.33	941	−0.31	959	−0.23
971	0.34	991	0.51	985	0.43	977	0.31	992	0.41	956	−0.02	938	−0.28	946	−0.24	964	−0.17
981	0.42	1002	0.64	994	0.54	986	0.43	1000	0.50	962	0.07	943	−0.23	952	−0.20	968	−0.12
989	0.53	1012	0.69	1005	0.61	997	0.50	1010	0.56	971	0.13	948	−0.15	956	−0.13	973	−0.07
999	0.60	1021	0.83	1015	0.71	1013	0.65			981	0.22	954	−0.12	962	−0.07	978	−0.01
1007	0.71			1023	0.79	1018	0.71			990	0.34	959	−0.05	966	−0.04	983	0.04
												963	−0.01	972	0.03	988	0.07
												967	0.03	976	0.07	993	0.12
												969	0.06	982	0.12	998	0.17
												974	0.10	986	0.16	1003	0.21

Table 2. Experimental Total Vapor Pressure, p_{tot}, above the Ternary Alloy $Ag_{42}Bi_{54}Sn_4$ (Alloy A)

run #1		run #2		run #3		run #4		run #5	
T/K	$\log(p_{tot}/Pa)$	T/K	$\log(p_{tot}/Pa)$	T/K	$\log(p_{tot}/Pa)$	T/K	$\log(p_{tot}/Pa)$	T/K	$\log(p_{tot}/Pa)$
923	−0.41	943	−0.27	923	−0.51	933	−0.51	953	−0.41
933	−0.30	953	−0.16	933	−0.41	943	−0.37	963	−0.30
943	−0.21	963	−0.05	943	−0.30	953	−0.27	973	−0.21
953	−0.09	973	0.06	953	−0.18	963	−0.16	983	−0.11
963	0.02	983	0.17	963	−0.09	973	−0.07	993	−0.03
973	0.09	993	0.29	973	0.02	983	0.02	1003	0.05
983	0.22	1003	0.37	983	0.12	993	0.13	1013	0.16
993	0.32	1013	0.47	993	0.21	1003	0.22	1023	0.24
1003	0.43	1023	0.55	1003	0.29	1013	0.30	1033	0.32
1013	0.54	1033	0.64	1013	0.39	1023	0.39	1043	0.41
1023	0.62	1043	0.72	1023	0.48	1033	0.47		
1033	0.72			1033	0.57	1043	0.56		
1043	0.82					1053	0.63		
						1063	0.72		

determined by vaporizing lead and cadmium, reference elements with well-known vapor pressures.[12] In the present work, in addition to lead, pure bismuth was also used as a reference. The temperature dependence of the total vapor pressure, p_{tot}, of this element was found in different sources,[12,14.15] and giving equal weight to the slopes and intercepts of the reported equations, the following relationship was selected

$$\log(p_{tot}/\mathrm{Pa}) = 10.58 - 9878/(T/\mathrm{K}) \qquad (1)$$

The average K_α obtained for bismuth in several runs ($K_\alpha = 14.6 \pm 0.2\ \mathrm{Pa{\cdot}rad^{-1}}$) agrees satisfactorily with the K_α values obtained for vaporizing lead ($K_\alpha = 14.5 \pm 0.3\ \mathrm{Pa{\cdot}rad^{-1}}$) and cadmium ($K_\alpha = 15.0 \pm 0.2\ \mathrm{Pa{\cdot}rad^{-1}}$), each one in a single run. Therefore, $K_\alpha = 14.6 \pm 0.2\ \mathrm{Pa{\cdot}rad^{-1}}$, obtained for Bi, was adopted to calculate the total vapor pressure above all the studied alloys. It is interesting to observe that no evident temperature dependence of K_α was observed during the vaporization of the reference elements, and this was taken as a check that no large errors in the temperature measurements occurred. The error associated with the average value of K_α produces an uncertainty of about ± 0.04 in the final $\log p_{tot}$ value. Consequently, this uncertainty affects the final value of the bismuth activity.

In the experimental temperature range, Bi(g) and Bi_2(g) are the predominant species present in the vapor above pure liquid bismuth and its liquid alloys, and as such, the Bi partial pressure, $\bar{p}_{Bi}$, at each experimental temperature was calculated from the measured total vapor pressure, p_{tot}, through the equilibrium constant, k_p of the process $2Bi(g) = Bi_2(g)$

$$k_p = (p_{tot} - \bar{p}_{Bi})p^\theta/\bar{p}_{Bi}^{\ 2} \qquad (2)$$

where $p^\theta = 10^5$ Pa is the standard pressure. The temperature dependence of k_p used in this work

$$\log k_p = A + BT + CT^2 + DT^3 \qquad (3)$$

[where $A = (35.4 \pm 0.3)$, $B = (-7.42 \pm 0.09)\cdot10^{-2}\ \mathrm{K^{-1}}$, $C = (5.3 \pm 0.1)\cdot10^{-5}\ \mathrm{K^{-2}}$, and $D = (-1.41 \pm 0.03)\cdot10^{-8}\ \mathrm{K^{-3}}$] was found through a polynomial best fitting of the literature data.[13,14,16] The pressures are expressed in pascals. The bismuth activity, a_{Bi}, in the liquid alloy was determined as the ratio between the Bi partial pressure above the molten alloy and that above the pure liquid element, both of course at the same temperature.

3. Results

One binary alloy, $Ag_{10}Bi_{90}$, and three ternary alloys, $Ag_{42}Bi_{54}Sn_4$, $Ag_{10}Bi_{88}Sn_2$, and $Ag_{30}Bi_{60}Sn_{10}$ (alloy A, B, and C, respectively), were studied. The bismuth activities were determined in each alloy at different bismuth compositions maintaining a constant ratio of X_{Sn}/X_{Ag} in the original ternary alloys. Because the vaporization of tin and silver is decidedly negligible compared to bismuth, the composition of an alloy could be changed by vaporizing controlled amounts of bismuth in different steps of an experiment. The measurements were carried out by increasing the temperature stepwise. The length of each isothermal step was kept as short as possible in such a way as to measure a sufficient number of values of torsion angles for the best accuracy and to avoid any evident change in the alloy composition. At the end of each run, some vapor pressures were measured, cooling the sample at temperatures comparable with those at the beginning of the vaporization. The reproducibility

Table 3. Experimental Total Vapor Pressure, p_{tot}, above the Ternary Alloy $Ag_{10}Bi_{88}Sn_2$ (Alloy B)

run #1		run #2		run #3		run #4		run #5		run #6		run #7		run #8		run #9	
T/K	log(p_{tot}/Pa)	T/K	log(p_{tot}/Pa)	T/K	log(p_{tot}/Pa)	T/K	log(p_{tot}/Pa)	T/K	log(p_{tot}/Pa)	T/K	log(p_{tot}/Pa)	T/K	log(p_{tot}/Pa)	T/K	log(p_{tot}/Pa)	T/K	log(p_{tot}/Pa)
898	−0.56	903	−0.56	903	−0.59	903	−0.67	938	−0.37	943	−0.37	933	−0.53	933	−0.56	933	−0.77
903	−0.53	908	−0.50	908	−0.53	908	−0.59	943	−0.33	948	−0.33	938	−0.47	938	−0.50	943	−0.67
908	−0.47	913	−0.44	913	−0.47	913	−0.53	948	−0.26	953	−0.26	943	−0.42	943	−0.44	953	−0.53
913	−0.42	918	−0.37	918	−0.39	918	−0.47	953	−0.20	958	−0.20	948	−0.37	948	−0.39	963	−0.44
918	−0.33	923	−0.31	923	−0.35	923	−0.42	958	−0.14	963	−0.13	953	−0.29	953	−0.33	973	−0.33
923	−0.26	928	−0.26	928	−0.29	928	−0.37	963	−0.09	968	−0.07	958	−0.24	958	−0.29	983	−0.26
928	−0.23	933	−0.20	933	−0.24	933	−0.29	968	−0.03	973	−0.01	963	−0.20	963	−0.23	993	−0.15
933	−0.14	938	−0.12	938	−0.15	938	−0.24	973	0.03	978	0.03	968	−0.12	968	−0.17	1003	−0.07
938	−0.09	943	−0.05	943	−0.08	943	−0.20	978	0.07	983	0.07	973	−0.07	973	−0.12	1013	0.02
943	−0.01	948	−0.01	948	−0.05	948	−0.12	983	0.13	988	0.13	978	−0.01	978	−0.06	1023	0.09
948	0.03	953	0.06	953	0.03	953	−0.07	988	0.17	993	0.18	983	0.03	983	−0.01		
953	0.10	958	0.10	958	0.07	958	−0.03	993	0.24	998	0.23	988	0.09	988	0.03		
958	0.15	963	0.17	963	0.13	963	0.04	998	0.29	1003	0.28	993	0.13	993	0.07		
963	0.21	968	0.22	968	0.17	968	0.09	1003	0.33	1008	0.34	998	0.18	998	0.12		
968	0.24	973	0.26	973	0.24	973	0.13	1008	0.36	1013	0.38	1002	0.23				
973	0.28	978	0.32	978	0.29	978	0.18	1013	0.43	1018	0.43	1008	0.29				
978	0.36	983	0.38	983	0.34	983	0.24	1018	0.47	1023	0.51	1013	0.33				
983	0.43	988	0.43	988	0.38	988	0.28	1023	0.53	1028	0.54	1018	0.39				
988	0.45	993	0.48	993	0.45			1028	0.58	1033	0.56	1023	0.42				
993	0.51	998	0.53	998	0.49			1033	0.62	1038	0.61	1028	0.46				
998	0.55	1003	0.58	1003	0.55			1038	0.67	1043	0.65	1033	0.51				
1003	0.61	1008	0.62	1008	0.61			1043	0.71	1048	0.70	1051	0.67				
1008	0.65	1014	0.70	1013	0.65												
1014	0.71	1018	0.72	1018	0.69												
1018	0.74	1023	0.78	1023	0.73												
1023	0.80	1028	0.82														
1028	0.83	1033	0.88														
1033	0.90	1038	0.92														

Table 4. Experimental Total Vapor Pressure, p_{tot}, above the Ternary Alloy $Ag_{30}Bi_{60}Sn_{10}$ (Alloy C)

run #1		run #2		run #3		run #4		run #5		run #6		run #7		run #8		run #9	
T/K	log(p_{tot}/Pa)	T/K	log(p_{tot}/Pa)	T/K	log(p_{tot}/Pa)	T/K	log(p_{tot}/Pa)	T/K	log(p_{tot}/Pa)	T/K	log(p_{tot}/Pa)	T/K	log(p_{tot}/Pa)	T/K	log(p_{tot}/Pa)	T/K	log(p_{tot}/Pa)
903	−0.67	903	−0.67	918	−0.53	918	−0.50	928	−0.53	913	−0.77	913	−0.77	933	−0.59	943	−0.59
908	−0.59	913	−0.56	923	−0.47	923	−0.47	933	−0.47	918	−0.67	918	−0.67	938	−0.53	948	−0.53
913	−0.53	918	−0.47	928	−0.37	928	−0.39	938	−0.42	923	−0.63	923	−0.63	943	−0.47	953	−0.50
918	−0.50	923	−0.42	933	−0.33	933	−0.33	943	−0.33	928	−0.56	928	−0.59	948	−0.44	958	−0.42
923	−0.42	928	−0.35	938	−0.26	938	−0.29	948	−0.29	933	−0.53	933	−0.53	953	−0.37	963	−0.37
928	−0.35	933	−0.29	943	−0.20	943	−0.23	953	−0.23	938	−0.44	938	−0.47	958	−0.33	968	−0.33
933	−0.29	938	−0.23	948	−0.17	948	−0.17	958	−0.17	943	−0.37	943	−0.37	963	−0.28	973	−0.29
938	−0.23	943	−0.17	953	−0.12	953	−0.12	963	−0.09	948	−0.33	948	−0.35	968	−0.23	978	−0.26
943	−0.17	948	−0.12	958	−0.05	958	−0.07	968	−0.05	953	−0.26	953	−0.29	973	−0.20	983	−0.20
948	−0.12	953	−0.05	963	0.01	963	0.01	973	0.03	958	−0.20	958	−0.24	978	-−0.12	988	−0.17
953	−0.05	958	0.01	968	0.06	968	0.04	978	0.07	963	−0.14	963	−0.20	983	−0.07	993	−0.12
958	0.03	963	0.06	973	0.12	973	0.09	983	0.13	968	−0.09	968	−0.14	988	−0.03	998	−0.07
963	0.07	968	0.10	978	0.17	978	0.12	988	0.17	973	−0.03	973	−0.07	993	0.03	1003	−0.01
968	0.13	973	0.18	983	0.22	983	0.18	993	0.23	978	0.03	978	−0.03	998	0.07	1008	0.04
973	0.21	978	0.22	988	0.29	988	0.23	998	0.27	983	0.09	983	0.03	1003	0.12	1013	0.07
978	0.24	983	0.28	993	0.33	993	0.29	1003	0.33	988	0.12	988	0.07	1008	0.16	1018	0.12
983	0.31	988	0.33	998	0.36	998	0.33	1008	0.37	993	0.18	993	0.12	1013	0.22	1023	0.17
988	0.33	993	0.37	1003	0.41	1003	0.38	1013	0.42	998	0.22	998	0.16	1018	0.25	1028	0.21
993	0.40	998	0.41	1008	0.45	1008	0.41	1018	0.45	1003	0.28	1003	0.22	1023	0.30	1033	0.25
998	0.43	1003	0.46	1013	0.50	1013	0.46	1023	0.51	1008	0.31	1008	0.27	1028	0.33	1038	0.29
1003	0.49	1008	0.49	1018	0.54	1018	0.50	1028	0.54	1013	0.36	1013	0.31	1033	0.36	1043	0.33
1008	0.55	1013	0.55	1023	0.58	1023	0.54	1033	0.58	1018	0.39	1018	0.33	1038	0.43	1048	0.39
1013	0.57	1018	0.58	1028	0.62	1028	0.58	1038	0.61	1023	0.45	1023	0.40	1043	0.47	1053	0.44
1018	0.61	1023	0.62	1033	0.67	1033	0.62	1043	0.65	1028	0.48	1028	0.43			1058	0.47
1023	0.66	1028	0.67			1038	0.66			1033	0.52	1033	0.47				
		1033	0.71														

of the values was taken as a check that no appreciable variation of the composition had occurred during the experiment. To verify the original composition of each alloy and the composition in bismuth, at the end of the vaporization runs, the sample was heated at higher temperatures to vaporize all residual bismuth. When this component was completely vaporized, the rotation of the cell at these temperatures was not detectable, and this confirmed that the vaporization of the other two components during the pressure measurements was decidedly negligible. The weights of the residues showed that the nominal compositions in bismuth of the alloys studied were equal within 0.5 % of the atomic % of Bi compared to the nominal ones. The total vapor pressure above the different alloys formed in each step was measured at different temperatures (see Tables 1 to 4). Their exact compositions were evaluated at the beginning and end of the pressure measurements. By the linear least-squares treatment of the experimental data, a log p_{tot} vs $1/T$ equation was obtained for each alloy (see Table 5), the composition of which is given as the average composition.

The bismuth activities in the liquid alloys were determined at 1000 K as the ratio between the Bi(g) partial pressures, calculated according to eq 2, and through the equations in Table 5, and the Bi(g) partial pressure above the pure element was calculated from eqs 1 and 2 [$\bar{p}_{Bi}(1000\ K) = 0.186\ Pa$)]. The results so obtained are reported in Table 6, and those referring to the binary alloy Ag−Bi are plotted in Figure 1 and compared, both at the same temperature (1000 K), with literature data.[17] The bismuth activities vs Bi atom % in ternary alloys are plotted in Figure 2.

Table 5. Temperature Dependence of the Total Vapor Pressure above Binary Alloy $Ag_{10}Bi_{90}$ and Ternary Alloys $Ag_{42}Bi_{54}Sn_4$ (A), $Ag_{10}Bi_{88}Sn_2$ (B), and $Ag_{30}Bi_{60}Sn_{10}$ (C)

		at % Bi			ΔT		$\log(p_{tot}/\mathrm{Pa}) = \mathrm{A} - \mathrm{B}/(T/\mathrm{K})$	
original alloy	run	initial	final	av	K	no. of points	A	B
$Ag_{10}Bi_{90}$	1	90	89.7	89.9	876−1007	13	10.54 ± 0.10	9917 ± 91
	2	86.8	86.2	86.5	909−1021	12	11.02 ± 0.26	10398 ± 248
	3	81.9	81.3	81.6	905−1023	13	10.05 ± 0.13	9470 ± 124
	4	74.2	73.5	73.9	895−1018	13	10.52 ± 0.13	9983 ± 127
	5	65.5	64.5	65.0	907−1010	11	10.30 ± 0.22	9798 ± 207
	6	53.9	53	53.5	880−990	13	9.99 ± 0.17	9558 ± 161
	7	43.7	43	43.4	907−974	17	10.09 ± 0.17	9722 ± 155
	8	38.1	37.2	37.7	895−986	17	10.38 ± 0.16	10062 ± 148
	9	30.8	29.7	30.3	922−1003	17	9.84 ± 0.11	9643 ± 103
A	1	53.9	53.6	53.8	923−1043	6	10.30 ± 0.10	9906 ± 94
	2	43.2	42.1	42.7	943−1043	11	10.11 ± 0.12	9780 ± 116
	3	34.7	33.8	34.3	923−1033	12	9.61 ± 0.06	9344 ± 62
	4	28.5	27.1	27.8	933−1063	14	9.38 ± 0.08	9195 ± 81
	5	20.1	19.4	19.8	953−1043	10	9.01 ± 0.09	8976 ± 86
B	1	75.9	75.3	75.6	898−1033	28	10.69 ± 0.07	10117 ± 66
	2	71.7	70.9	71.3	903−1038	28	10.84 ± 0.04	10287 ± 42
	3	62.6	63.3	63.0	903−1023	25	10.80 ± 0.06	10287 ± 53
	4	50.7	50.2	50.5	903−988	18	10.37 ± 0.08	9953 ± 76
	5	41	40.3	40.7	938−1043	22	10.43 ± 0.06	10127 ± 55
	6	35.1	34.6	34.9	943−1048	22	10.36 ± 0.09	10112 ± 89
	7	31.2	30.4	30.8	933−1051	22	10.26 ± 0.07	10058 ± 70
	8	26.6	26	26.3	933−998	14	9.96 ± 0.10	9811 ± 93
	9	12.6	11.9	12.3	933−1023	10	9.05 ± 0.17	9149 ± 169
C	1	55.0	54.6	54.8	903−1023	25	10.85 ± 0.10	10390 ± 92
	2	50.2	49.6	49.9	903−1033	26	10.37 ± 0.10	9946 ± 97
	3	44.9	44.3	44.6	918−1033	24	10.16 ± 0.09	9785 ± 91
	4	39.9	39.2	39.6	918−1038	25	9.66 ± 0.07	9318 ± 68
	5	35.1	34.3	34.7	928−1043	24	10.37 ± 0.12	10090 ± 122
	6	29.8	29.0	29.4	913−1033	25	10.39 ± 0.11	10160 ± 105
	7	25.3	24.6	25.0	913−1033	25	9.87 ± 0.08	9693 ± 79
	8	20.0	19.5	19.8	933−1043	23	9.43 ± 0.06	9342 ± 61
	9	14.5	13.7	14.1	943−1063	25	9.09 ± 0.06	9125 ± 63

4. Discussion

The second-law partial molar vaporization enthalpy, $\overline{\Delta_v H_T}(\mathrm{Bi})$, related to the process

$$\text{alloy(l)} \rightarrow \text{Bi(g)} + \text{alloy(l)} \tag{4}$$

was calculated from the slopes of log $\bar{p}_{Bi}$ vs $1/T$ equations reported in Table 5 at different alloy compositions. Reaction 4 is consistent when considering that the composition of the molten alloy is practically constant during the measurements carried out in each run because of the very negligible amount of bismuth that vaporized with respect to the amount of alloy employed. Combining this enthalpy with the vaporization enthalpy of pure molten bismuth, $\Delta_v H^\theta_T(\mathrm{Bi})$ [$\Delta_v H^\theta_{1000}(\mathrm{Bi}) = 192.282\ \mathrm{kJ{\cdot}mol^{-1}}$],[12] the partial enthalpy, $\overline{\Delta_{mix} H_T}(\mathrm{Bi})$, associated with the mixing of one mole of liquid bismuth in a molten alloy, according to the equation

$$\text{Bi(l)} + \text{alloy(l)} = \text{alloy(l)} \tag{5}$$

was calculated as

$$\overline{\Delta_{mix} H_T}(\mathrm{Bi}) = \Delta_v H^\theta_T(\mathrm{Bi}) - \overline{\Delta_v H_T}(\mathrm{Bi}) \tag{6}$$

Furthermore, using the bismuth activities reported in Table 4, the partial mixing molar quantities

$$\overline{\Delta_{mix} G_T}(\mathrm{Bi}) = RT \ln a_{Bi} \tag{7}$$

and, consequently

$$\overline{\Delta_{mix} S_T}(\mathrm{Bi}) = [\overline{\Delta_{mix} H_T}(\mathrm{Bi}) - RT \ln a_{Bi}]/T \tag{8}$$

were calculated. The values of these quantities at 1000 K are reported in Table 7.

The excess integral free-energy change for the mixing, $\Delta_{mix}G_T(\mathrm{xs})$, in a ternary alloy can be evaluated using one of the methods of solving the Gibbs−Duhem equation proposed in the literature. When a set of activity data is available for only one component and the ratio, ρ, between the compositions of the other two components is constant, the Darken equation[18] can be used. In the present study, it is written as

$$\Delta_{mix}G_T(\mathrm{xs}) = (1 - X_{Bi}) \int_1^{x_{Bi}} [\alpha_{Bi} dX_{Bi}]_\rho - X_{Sn} \int_1^0 [\alpha_{Bi} dX_{Bi}]_{X_{Ag}=0} - X_{Ag} \int_1^0 [\alpha_{Bi} dX_{Bi}]_{X_{Sn}=0} \tag{9}$$

where $\rho = X_{Sn}/X_{Ag}$ and α_{Bi} is given by

$$\alpha_{Bi} = RT(1 - X_{Bi})^{-2} \ln(a_{Bi}/X_{Bi}) \tag{10}$$

The second and third integrals on the right-hand side of eq 9 are referred to the α_{Bi} in the binary Bi−Sn and Ag−Bi systems, respectively. Equation 9 can be simply integrated for the ternary system in which all the solutions are strictly regular;[19] that is, α_{Bi} remains constant along any given integration path with ρ fixed. The binary Bi−Sn and Ag−Bi systems must also be regular. To check this, α_{Bi} has been calculated for the ternary system, using the present experimental data given in Figure 2 and Table 6, and for the binary alloys, using literature data.[17] Figure 3 shows that neither the binary nor the ternary systems are strictly regular solutions, particularly the Ag−Bi system. The binary system Bi−Sn is considered regular[17] ($\Delta_{mix}H_{600} = 58 \pm 42\ \mathrm{J{\cdot}mol^{-1}}$), and this has been confirmed recently[20]

Table 6. Bi(g) Partial Pressures, $\bar{p}_{Bi}$, at 1000 K above Binary Alloy $Ag_{90}Bi_{10}$ and Ternary Alloys $Ag_{42}Bi_{54}Sn_4$ (A), $Ag_{10}Bi_{88}Sn_2$ (B), and $Ag_{30}Bi_{60}Sn_{10}$ (C)[a]

			$\log(\bar{p}_{Bi}/Pa) = A - B/(T/K)$		$\bar{p}_{Bi}$ at 1000 K	
original alloy	run	at % Bi average	A	B	Pa	a_{Bi}
$Ag_{10}Bi_{90}$	1	89.9	10.29 ± 0.06	10146 ± 54	1.385	0.90
	2	86.5	10.57 ± 0.15	10434 ± 149	1.379	0.90
	3	81.6	10.00 ± 0.08	9884 ± 75	1.304	0.85
	4	73.9	10.28 ± 0.08	10193 ± 77	1.236	0.81
	5	65.0	10.18 ± 0.13	10108 ± 124	1.176	0.77
	6	53.5	9.99 ± 0.11	9965 ± 99	1.069	0.70
	7	43.4	10.07 ± 0.10	10081 ± 96	0.980	0.64
	8	36.7	10.29 ± 0.09	10322 ± 89	0.921	0.60
	9	30.3	10.01 ± 0.07	10120 ± 63	0.771	0.50
A	1	53.8	10.14 ± 0.06	10134 ± 59	1.011	0.66
	2	42.7	10.08 ± 0.07	10115 ± 68	0.925	0.60
	3	34.3	9.74 ± 0.04	9818 ± 37	0.844	0.55
	4	27.8	9.64 ± 0.05	9770 ± 48	0.744	0.48
	5	19.8	9.39 ± 0.06	9615 ± 60	0.595	0.39
B	1	75.6	10.38 ± 0.04	10264 ± 40	1.299	0.85
	2	71.3	10.47 ± 0.03	10376 ± 25	1.255	0.82
	3	63.0	10.39 ± 0.04	10314 ± 34	1.182	0.77
	4	50.5	10.20 ± 0.05	10183 ± 47	1.037	0.68
	5	40.7	10.32 ± 0.03	10377 ± 34	0.886	0.58
	6	34.9	10.28 ± 0.05	10363 ± 50	0.820	0.53
	7	30.8	10.24 ± 0.04	10360 ± 37	0.766	0.50
	8	26.3	10.02 ± 0.06	10165 ± 61	0.712	0.46
	9	12.3	9.46 ± 0.11	9771 ± 111	0.488	0.32
C	1	54.8	10.47 ± 0.06	10432 ± 57	1.101	0.72
	2	49.9	10.19 ± 0.06	10164 ± 60	1.051	0.68
	3	44.6	10.06 ± 0.06	10067 ± 56	0.981	0.64
	4	39.6	9.75 ± 0.04	9784 ± 41	0.928	0.60
	5	34.7	10.22 ± 0.07	10285 ± 74	0.852	0.56
	6	29.4	10.24 ± 0.07	10338 ± 64	0.799	0.52
	7	25.0	9.90 ± 0.05	10031 ± 48	0.738	0.48
	8	19.8	9.60 ± 0.04	9794 ± 39	0.636	0.41
	9	14.1	9.41 ± 0.05	9690 ± 49	0.527	0.34

[a] The bismuth activity at 1000 K is given in the rightmost column. Bi(g) partial pressure above pure bismuth is equal to 0.186 Pa.[12] The quoted errors are standard deviations.

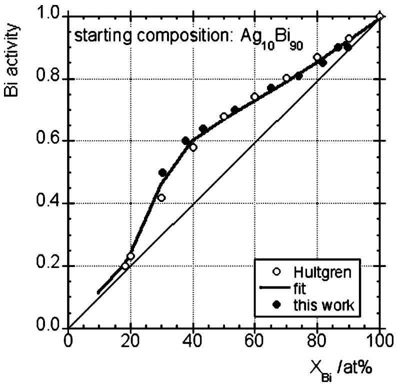

Figure 1. Bi activity determined as a function of atomic fraction of Bi, X_{Bi}, in the binary alloy at the original composition $Ag_{10}Bi_{90}$. Data are compared with the literature.[17]

($\Delta_{mix}H_{723}$ = 93 J·mol^{-1}). Therefore, simplified versions of eq 9 cannot be used.

Looking at the curves of Figure 3, it appears clearly that α_{Bi} is always positive in the whole X_{Bi} interval. According to eq 10, this implies that the Bi activity coefficient, γ_{Bi}, is always greater than 1 for both the binary and ternary systems. On the other hand, this is experimentally consistent with data reported in Figures 1 and 2 where the deviations from the ideal behavior of Bi are always positive.

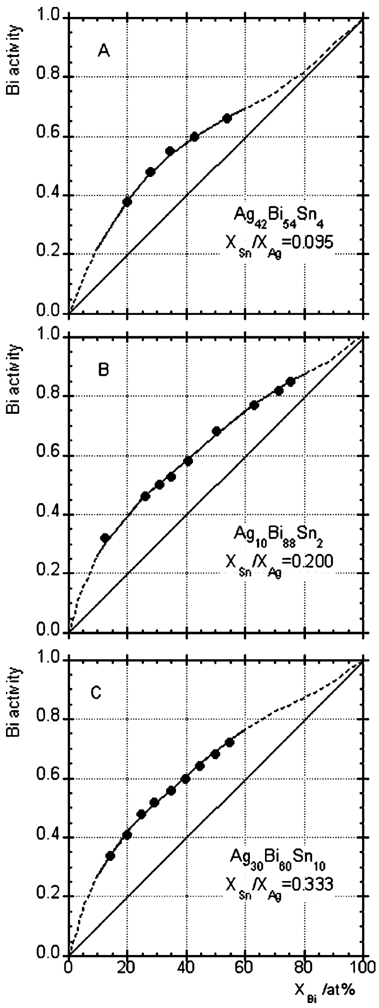

Figure 2. Bi activity determined as a function of atomic fraction of Bi, X_{Bi}, in ternary alloys at original compositions: A ≡ $Ag_{42}Bi_{54}Sn_4$, B ≡ $Ag_{10}Bi_{88}Sn_2$, C ≡ $Ag_{30}Bi_{60}Sn_{10}$.

The values of the mixing integral free energy of excess, $\Delta_{mix}G_T(xs)$, given by eq 9 and the mixing integral free energy of the real solution, $\Delta_{mix}G_T(re)$, are reported in Figure 4 and in Table 7.

By definition, $\Delta_{mix}G_T(re)$ is given by

$$\Delta_{mix}G_T(re) = \Delta_{mix}G_T(xs) + RT\sum_i X_i \ln X_i \tag{11}$$

Figure 4 shows that the condition of the ideal solution, i.e., $\Delta_{mix}G_T(xs) = 0$, is found at $\rho = 0.095$ and $X_{Bi} = 0.2$ and at $X_{Bi} = 0.5$ when the values of ρ are equal to 0.200 and 0.333.

$\Delta_{mix}G_T(xs)$ data can be independently checked by comparing the binary Ag−Sn portion of the ternary alloys under study with the data of the Ag−Sn binary alloy from the literature.[17] The quantity $\Delta_{mix}G_T(xs)$ can be decomposed as

$$\left[\frac{\Delta_{mix}G_T(xs)}{RT} - X_{Bi}\ln(a_{Bi}/X_{Bi})\right] = (X_{Ag}\ln\gamma_{Ag} + X_{Sn}\ln\gamma_{Sn}) \tag{12}$$

where γ are the activity coefficients. The right side of eq 12 corresponds to $\Delta_{mix}G_T(xs)_{Ag-Sn}/RT$, $\Delta_{mix}G_T(xs)_{Ag-Sn}$ being the excess mixing integral free energy of Ag−Sn binary alloys. Everything on the left side of eq 12 is known. Figure 5 displays the quantity $(X_{Ag}\ln\gamma_{Ag} + X_{Sn}\ln\gamma_{Sn})$ vs ρ. The solid line refers to the Ag−Sn system as reported in the literature.[17] At fixed ρ (see magnified inset in Figure 5), there is at least one ternary

Table 7. Partial Mixing Molar Quantities $\overline{\Delta_{\mathrm{mix}}G_{\mathrm{T}}}$(Bi), $\overline{\Delta_{\mathrm{mix}}H_{\mathrm{T}}}$(Bi), and $\overline{\Delta_{\mathrm{mix}}S_{\mathrm{T}}}$(Bi) and Integral Mixing Free Energy of Excess, $\Delta_{\mathrm{mix}}G_{\mathrm{T}}$(xs), and Real Solutions, $\Delta_{\mathrm{mix}}G_{\mathrm{T}}$(re)[a]

alloy	# run	X_{Bi}	X_{Ag}	X_{Sn}	a_{Bi}	$\overline{\Delta_{\mathrm{mix}}G_{\mathrm{T}}}$(Bi) kJ·mol^{-1}	$\overline{\Delta_{\mathrm{mix}}H_{\mathrm{T}}}$(Bi) kJ·mol^{-1}	$\overline{\Delta_{\mathrm{mix}}S_{\mathrm{T}}}$(Bi) J·mol^{-1}·K^{-1}	$\Delta_{\mathrm{mix}}G_{\mathrm{T}}$(xs) kJ·mol^{-1}	$\Delta_{\mathrm{mix}}G_{\mathrm{T}}$(re) kJ·mol^{-1}
A	1	0.538	0.422	0.040	0.66	−3.5 ± 0.6	−2 ± 1	2 ± 1	1.2	−5.7
	2	0.427	0.524	0.050	0.60	−4.2 ± 0.7	0 ± 1	4 ± 1	1.0	−6.1
	3	0.343	0.600	0.057	0.55	−5.0 ± 0.8	4.3 ± 0.7	9.0 ± 0.9	0.73	−6.2
	4	0.278	0.659	0.063	0.48	−6.1 ± 0.9	5.2 ± 0.9	11 ± 1	0.45	−6.2
	5	0.198	0.733	0.070	0.38	−8.0 ± 1.1	8 ± 1	16 ± 2	0.00	−6.1
B	1	0.756	0.377	0.075	0.72	−2.7 ± 0.6	−4.2 ± 0.8	−1.8 ± 0.9	0.3	−7.1
	2	0.713	0.417	0.083	0.68	−3.2 ± 0.6	−6.3 ± 0.5	−3.4 ± 0.6	0.0	−7.6
	3	0.630	0.462	0.092	0.64	−3.7 ± 0.6	−5.2 ± 0.6	−1.5 ± 0.8	−0.3	−8.1
	4	0.505	0.504	0.101	0.60	−4.2 ± 0.7	−2.7 ± 0.9	2 ± 1	−0.7	−8.5
	5	0.407	0.544	0.109	0.56	−4.8 ± 0.7	−6.4 ± 0.6	−1.6 ± 0.8	−1.1	−8.9
	6	0.349	0.588	0.118	0.52	−5.4 ± 0.8	−6 ± 1	−1 ± 1	−1.6	−9.3
	7	0.308	0.625	0.125	0.48	−6.1 ± 0.9	−6.0 ± 0.7	0 ± 1	−2.1	−9.6
	8	0.263	0.669	0.134	0.41	−7 ± 1	−2 ± 1	5 ± 1	−2.7	−9.9
	9	0.123	0.716	0.143	0.34	−9 ± 1	5 ± 2	14 ± 2	−3.5	−10
C	1	0.548	0.183	0.061	0.85	−1.3 ± 0.5	−7 ± 1	−6 ± 1	0.7	−5.1
	2	0.499	0.215	0.072	0.82	−1.6 ± 0.5	−2 ± 1	−1 ± 1	0.7	−5.7
	3	0.446	0.278	0.092	0.77	−2.2 ± 0.5	−4 ± 1	−2 ± 1	0.5	−6.7
	4	0.396	0.371	0.124	0.68	−3.2 ± 0.6	5.0 ± 0.7	8.2 ± 0.9	0.1	−8.0
	5	0.347	0.445	0.148	0.58	−4.5 ± 0.7	−6 ± 1	−1 ± 1	−0.5	−8.9
	6	0.294	0.488	0.163	0.53	−5.3 ± 0.8	−6 ± 1	0 ± 1	−0.9	−9.3
	7	0.250	0.519	0.173	0.50	−5.8 ± 0.8	0 ± 1	6 ± 1	−1.2	−9.6
	8	0.198	0.553	0.184	0.46	−6.5 ± 0.9	4.8 ± 0.7	11.0 ± 0.9	−1.7	−9.9
	9	0.141	0.658	0.219	0.32	−10 ± 1	6.8 ± 0.9	16 ± 1	−3.2	−10

[a] All the values were calculated at $T = 1000$ K. A ≡ $Ag_{42}Bi_{54}Sn_4$, B ≡ $Ag_{10}Bi_{88}Sn_2$, C ≡ $Ag_{30}Bi_{60}Sn_{10}$ are the original compositions of the alloys studied.

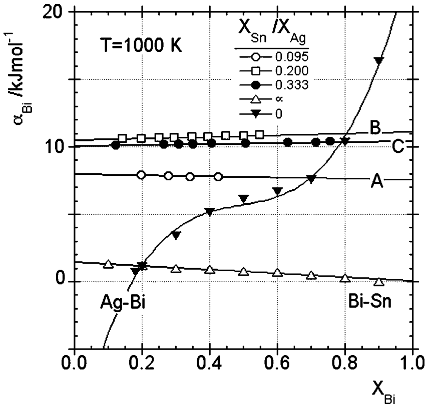

Figure 3. Curves representing the values of α_{Bi} vs X_{Bi} calculated according to eq 10 at $T = 1000$ K. The curves related to the binary alloys Bi−Sn ($\rho = \infty$) and Ag−Bi ($\rho = 0$) have been calculated by using literature data.[14]

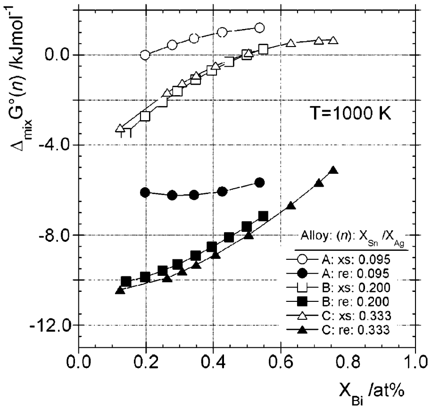

Figure 4. Calculated curves of excess (n = xs) and real (n = re) mixing integral free energies, $\Delta_{\mathrm{mix}}G_{\mathrm{T}}(n)$, as a function of X_{Bi}. The curves have been calculated by eq 9 and eq 11, respectively.

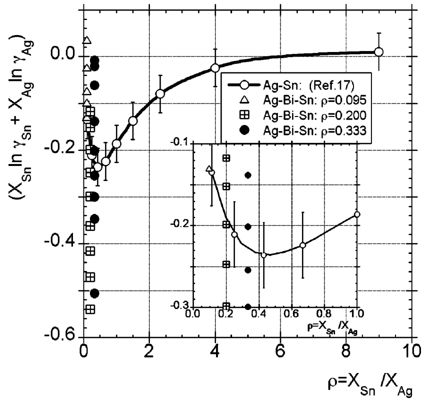

Figure 5. Comparison of the binary component ($X_{\mathrm{Ag}} \ln \gamma_{\mathrm{Ag}} + X_{\mathrm{Sn}} \ln \gamma_{\mathrm{Sn}}$) in $\Delta_{\mathrm{mix}}G_{\mathrm{T}}$(xs) of the ternary alloys with the same term in the binary system Ag−Sn calculated from the literature.[14] The magnification in the inset displays the comparison in a ρ interval closer to the investigated ρ values.

alloy at a given Bi composition, the behavior of which is equal to the behavior of a Ag−Sn binary alloy having the same ρ. In these conditions, this means that the presence of Bi does not produce any kind of interaction. Some similar findings can be observed in Figure 6 where at certain Bi compositions the Bi activity is practically independent of ρ (see, particularly, $X_{\mathrm{Bi}} = 0.4$).

The mixing partial molar quantities of Bi, reported in Table 7, show that their degree of internal consistency depends more on the temperature dependency of the actual p_{Bi} measurement run than on the single p_{Bi} measurement, i.e., the single a_{Bi} value. In fact, a regular trend is found for $\overline{\Delta_{\mathrm{mix}}G_{\mathrm{T}}}$(Bi), whereas a more scattered behavior is found for $\overline{\Delta_{\mathrm{mix}}H_{\mathrm{T}}}$(Bi). This also produces some effects on $\overline{\Delta_{\mathrm{mix}}S_{\mathrm{T}}}$(Bi) through the application of eq 8. It is worth noticing that eq 6 can be rewritten in the form

$$R\left[\frac{\partial \ln \gamma_{\mathrm{Bi}}}{\partial(1/T)}\right]_{X_{\mathrm{Bi}},\rho} = \overline{\Delta_{\mathrm{mix}}H_{\mathrm{T}}}(\mathrm{Bi}) = [\Delta_{\mathrm{v}}H^{\theta}_{\mathrm{T}}(\mathrm{Bi}) - \overline{\Delta_{\mathrm{v}}H_{T}}(\mathrm{Bi})] \tag{13}$$

Thus, the value of $\overline{\Delta_{\mathrm{v}}H_{\mathrm{T}}}$(Bi) and, consequently $\overline{\Delta_{\mathrm{mix}}H_{\mathrm{T}}}$(Bi), is a function strictly depending on the alloy composition. The

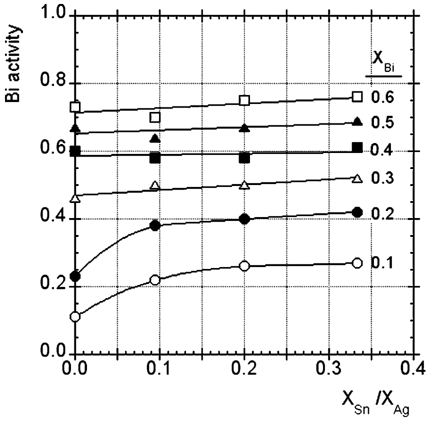

Figure 6. Bi activity vs ρ at increasing X_{Bi} values. This plot derives from Figures 1 and 2.

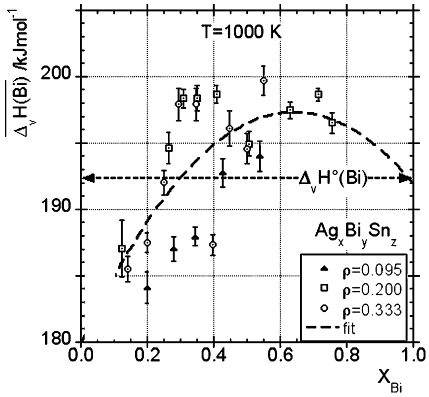

Figure 7. Cumulated $\overline{\Delta_{v}H_{T}}(\mathrm{Bi})$ values reported as a function of X_{Bi} for all the ternary alloys studied. The difference between each $\overline{\Delta_{v}H_{T}}(\mathrm{Bi})$ value and the standard vaporization enthalpy of pure Bi, $\Delta_{v}H^{\theta}_{T}(\mathrm{Bi})$, gives $\overline{\Delta_{\mathrm{mix}}H_{T}}(\mathrm{Bi})$, according to eq 6 or 13.

interactions among the components in the alloy can be modified even for negligible changes in the composition as it can occur during the vaporization of small quantities of Bi, as in the present experiments. All the values of $\overline{\Delta_{v}H_{T}}(\mathrm{Bi})$ vs X_{Bi}, measured for all the ternary alloys tested, are reported in Figure 7 at different ratios, ρ. The curve used to fit all the points divides the plot in two regions: above and below the standard enthalpy of vaporization of pure Bi, $\Delta_{v}H^{\theta}_{T}(\mathrm{Bi})$. Above this curve, $\overline{\Delta_{\mathrm{mix}}H_{T}}(\mathrm{Bi}) < 0$, and below the curve $\overline{\Delta_{\mathrm{mix}}H_{T}}(\mathrm{Bi}) > 0$. One can observe that on both sides, values at different ρ ratios are present, and the increase of X_{Bi} shifts $\overline{\Delta_{\mathrm{mix}}H_{T}}(\mathrm{Bi})$ toward more exothermic values. Of course, the presence of a maximum in the fitted curve is expected.

5. Conclusions

The thermodynamic characterization of some ternary alloys in the system Ag−Bi−Sn has been performed by Bi activity measurements making use of the torsion−effusion technique. Several thermodynamic quantities were evaluated at $T = 1000$ K. They are Bi mixing partial molar quantities such as $\overline{\Delta_{\mathrm{mix}}G_{T}}(\mathrm{Bi})$, $\overline{\Delta_{\mathrm{mix}}H_{T}}(\mathrm{Bi})$, and $\overline{\Delta_{\mathrm{mix}}S_{T}}(\mathrm{Bi})$ as well as mixing integral molar quantities, i.e., $\Delta_{\mathrm{mix}}G_{T}(\mathrm{xs})$ and $\Delta_{\mathrm{mix}}G_{T}(\mathrm{re})$. To the authors knowledge, no such data are present in the literature, and the present data may be found useful for a more accurate description of the thermodynamics of the Ag−Bi−Sn system.

Acknowledgment

The authors would like to thank Prof. G. Zanicchi of Dipartimento di Chimica e Chimica Industriale, Università di Genova, Italy, for the preparation and characterization of the alloy samples.

Literature Cited

(1) Lead-free Solder Materials, COST Action 531, http://www.univie.ac.at/cost531/.
(2) Brunetti, B.; Gozzi, D.; Iervolino, M.; Latini, A. Bismuth Activity in Lead-free Solder Bi-In-Sn alloys. *CALPHAD* **2006**, *30*, 431−2.
(3) Hassam, S.; Dichi, E.; Legendre, P. Experimental Equilibrium Phase Diagram of the Ag−Bi−Sn System. *J. Alloys Compd.* **1998**, *268*, 199−6.
(4) Garzel, G.; Zabdyr, L. A. Electromotive force study of the liquid silver−bismuth−tin alloys. *J. Phase Equilib. Diffusion* **2006**, *27*, 140−4.
(5) Doi, K.; Ohtani, H.; Hasebe, M. Thermodynamic study of the phase equilibria in the Sn−Ag−Bi−Cu quaternary system. *Mater. Trans.* **2004**, *45*, 380−3.
(6) Katayama, I; Tanaka, T.; Akai, S-I.; Yamazaki, K. Activity measurements of liquid Sn−Ag−Bi alloys by fused salt EMF method. *Mater. Sci. Forum* **2005**, *502*, 129−4.
(7) Terzieff, P.; Li, Z.; Knott, S.; Mikula, A. Physicochemical properties of liquid Ag−Bi−Sn. *Physica B* **2007**, *388*, 312−7.
(8) Hassam, S.; Gambino, M.; Bros, J. P. Enthalpy of formation of liquid silver−bismuth and silver−bismuth−tin alloys. *Z. Metallkd.* **1994**, *85*, 460−71.
(9) Kattner, U. R.; Boettinger, W. J. On the Sn−Bi−Ag ternary phase diagram. *J. Electron. Mater.* **1994**, *23*, 603−0.
(10) Ohtani, H.; Satoh, I.; Miyashaita, M.; Ishida, K. Thermodynamic analysis of the Sn−Ag−Bi ternary phase diagram. *Mater. Trans.* **2001**, *42*, 722−1.
(11) Brunetti, B.; Piacente, V.; Scardala, P. Torsion Vapor Pressures and Sublimation Enthalpies of Arsenic Triselenide and Tritelluride. *J. Chem. Eng. Data* **2007**, *52*, 24−9.
(12) Gurvich, L. V.; Yungman, V. S. *IVTANTHERMO Database of Thermodynamic Properties of Individual Substances and Thermodynamic Modeling Software*, version 3.0; Glushko Thermocenter of R. A. S.: 2005.
(13) Piacente, V.; Fontana, D.; Scardala, P. Enthalpies of Vaporization of a Homologous Series of *n*-Alkanes Determined from Vapor Pressure Measurements. *J. Chem. Eng. Data* **1994**, *39*, 231−7.
(14) Hultgren, R.; Desai, P. D.; Hawkins, D. T.; Gleiser, M.; Kelley, K. K.; Wagman, D. D. *Selected Values of the Thermodynamic Properties of the Elements*; American Society for Metals: Metals Park, OH, 1973.
(15) Kubashewski, O.; Ünal, H. An empirical estimation of the heat capacities of inorganic compounds. *High Temp.-High Press.* **1977**, *9*, 361−5.
(16) Yoshioka, H.; Tada, Y.; Kunimine, K.; Furuichi, T.; Hayashi, Y. Heat transfer and solidification processes of alloy melt with undercooling: II. Solidification model. *Acta Mater.* **2006**, *54*, 765−1.
(17) Hultgren, R.; Desai, P. D.; Hawkins, D. T.; Gleiser, M.; Kelley, K. K. *Selected Values of the Thermodynamic Properties of Binary Alloys*; American Society for Metals: Metals Park, OH, 1973.
(18) Darken, L. S. Application of the Gibbs−Duhem equation to ternary and multicomponent systems. *J. Am. Chem. Soc.* **1950**, *72*, 2909−14.
(19) Toop, G. W. Predicting ternary activities using binary data. *Trans. Met. Soc. AIME* **1965**, *233*, 850−5.
(20) Asryan, N.; Mikula, A. Thermodynamic properties of liquid Bi−Sn alloys. *Z. Metallkd.* **2004**, *95*, 132−5.

Received for review February 16, 2007. Accepted April 14, 2007. This work was performed in the framework of the E.C. action COST 531 project “Lead-free solder materials”.

JE7000914